

Learning Efficient Control of Robots Using Myoelectric Interfaces

Mark Ison, Chris Wilson Antuvan and Panagiotis Artemiadis

Abstract—Myoelectric controlled interfaces are a vital component for advancing applications in prostheses, exoskeletons, and robot teleoperation. Current methods search for optimal neural decoders for enhanced initial user performance. However, recent studies demonstrate learning an inverse model of abstract decoders to improve performance over time. This paper proposes a paradigm shift on myoelectric interfaces by embedding the human as controller of a system and allowing the human to *learn* how to control it via control tasks with similar mapping functions. The method is tested using two different control tasks and four different abstract mappings of upper limb myoelectric signals to control actions for those tasks. The results confirm that all subjects are able to learn the mappings and improve performance efficiency over time. A cross-trial evaluation reveals a significant learning transfer when a new control task is presented using the same mapping as a previous task, resulting in enhanced initial performance with the new task. Comparison of EMG signal evolution across subjects indicates a significant population-wide muscle synergy development that results from learning and implementing the inverse model of the mapping function to complete the tasks. This suggests that efficient performance may be achieved by learning a constant, arbitrary mapping function applied to multiple control tasks rather than dynamic subject- or task-specific functions. Moreover, this method can be used for the neural control of any device or robot, without restricting them to anthropomorphic or human-related counterparts.

I. INTRODUCTION

Myoelectric controlled interfaces, through mediating connections between electromechanical systems and humans, are a vital component for advancing applications in prostheses, orthoses, and robot teleoperation. This technology offers promise to help amputees regain independence [1], [2], humans perform tasks beyond their physical capabilities [3], [4], and robotic devices be teleoperated with precision [5], [6], [7], [8]. Breakthroughs in reliable detection of neural signals using electromyography (EMG) have given researchers noninvasive access to muscle activity, bringing myoelectric interfaces to the forefront for further advancement of these applications.

A. Neural Decoding

Current research has focused on improving performance of myoelectric controlled interfaces through optimal decoding of neural signals. Various algorithms use machine learning techniques, but wide inter-user variability in EMG signals requires intense training phases to create a decoder specifically for a given user [1], [2], [9], [10]. Even with

training, this highly non-linear system makes satisfactory decoding accuracy difficult to achieve [11]. Other methods use intuitive decoders to control an interface with a small set of simple commands, translating to predefined actions by a robot [12], [13]. However, the rigid set of actions limit users' ability to learn better control of the system, and the performance cannot generalize to new tasks. Both methods intend to maximize the initial performance of the user. This does not capitalize on a human's natural ability to learn and optimize control strategies while performing tasks [14]. Thus, these approaches may not provide a foundation for efficient performance over time.

Alternatively, other works investigate the capacity to learn an inverse model of a predefined decoding function. Héliot et. al [15] form a model of the brain to convert firing neurons to two dimensional (2D) positions for center to reach out tasks. This model simulates how minimizing output error influences brain plasticity to learn the inverse model of the decoding function. Kim et. al [16] confirm these results experimentally with closed loop training. Chase et. al [17], when comparing performance of two decoding algorithms, show significant performance differences between decoders in open loop tasks, but minimal difference in online closed loop control tasks.

Closed loop myoelectric controlled interfaces are further investigated by Radhakrishnan et. al [18] to understand human motor learning. Two distinct decoders are used to decode EMG signal amplitude from six muscles to generate a 2D cursor position. The intuitive decoder maps muscles to a vector along the 2D plane most consistent with limb movement when the muscle contracts. The non-intuitive decoder maps muscles randomly along equally spaced vectors in the plane. Results indicate learning via performance trends best fit by exponential decay. While the intuitive decoder gives better initial performance, the non-intuitive decoder provides a steeper learning rate and achieves nearly equal performance after 192 trials.

Pistohl et. al [19] demonstrate the natural extension of this motor learning to practical robotic applications. Using EMG signals to control fingers on a robotic hand, subjects are able to learn a non-intuitive decoding function with comparable performance to a 2D cursor control task similar to [18].

These studies establish that humans can learn to control myoelectric interfaces using various decoders when presented with closed-loop feedback. The study presented in this paper expands these findings by investigating the performance impact of previously learned mappings on new control tasks. In addition, population-wide muscle synergy development is evaluated to confirm learning of a more efficient control.

Mark Ison, Chris Wilson Antuvan and Panagiotis Artemiadis are with the School for Engineering of Matter, Transport and Energy, Arizona State University, Tempe, AZ 85287 USA

Email: {mison, cantuvan, panagiotis.artemiadis}@asu.edu

*Corresponding author.

Muscle synergies represent a series of muscle activation patterns used to achieve a behavioral goal. The Central Nervous System, instead of activating each individual muscle separately, activates a combination of muscle synergies to produce a desired motion [20]. Previous studies have identified synergies from EMG signals of a given user to simplify decoding of arm kinematics [21] and predict hand motions [9]. Synergies have also been associated with improved control during interaction with abstract decoding functions [22].

Before presenting the novelty of the proposed technique, two concepts frequently used in this paper are defined:

Control task

The task to be executed using myoelectric controls, implying both the *device* (e.g. a robot hand) and its possible *functions* (e.g. open/close fingers etc).

Mapping function

A mathematical function relating myoelectric activity to controls for the task (e.g. a function translating bicep EMG to opening the fingers of a robot hand).

B. Contribution

This paper proposes a paradigm shift on myoelectric interfaces by suggesting arbitrary mapping functions between the neural activity and the control actions that can be learned via alternative control tasks. More specifically, this paper investigates user performance efficiency and population synergy development with myoelectric interfaces and arbitrary mapping functions which were neither designed for the subject nor the task. Expanding on recent conclusions that visual feedback is effective for learning decoders in myoelectric interfaces [16], [17], [18], [19], this paper provides evidence that subjects do not only learn mappings between their actions and a specific control task, but they can retain this learning and generalize it to different control tasks having similar mapping functions. The implications of this contribution are vast, suggesting that efficient control of robots can be achieved through learning to control different myoelectric interfaces using similar mapping functions. To the best of the authors' knowledge, no other study has performed such an analysis to support the shift to human embedded control of devices using generalizable myoelectric interfaces.

II. METHODS

A. Experimental Setup

The experiments are designed to evaluate transfer of human motor learning across new control tasks and compare muscle synergy development across subjects. The setup for the experiment (shown in Fig. 1) includes wireless EMG sensors (Delsys Trigno Wireless, Delsys Inc), and a multi-function data acquisition card (DAQ) (USB-6343X, NI), which acquires the signal and sends it to a Personal Computer (PC). A C++ program processes the signal in real time and a mapping function transforms it into control outputs for performing the two tasks. The tasks are displayed on the monitor via OpenGL API [23] to provide visual feedback.

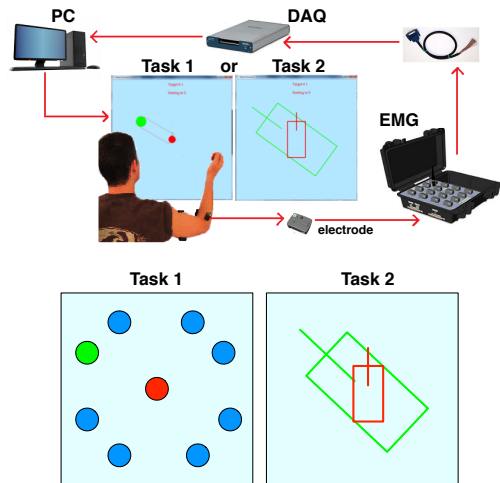


Fig. 1. Experimental setup includes an EMG system, DAQ, and visual interface (top). The two tasks the subjects control using EMG signals (bottom).

B. Control Tasks

Two distinct tasks provide different visual feedback for the subject (see Fig. 1). The goal of each task is to transition a virtual object from its initial state to one of eight target states as quickly as possible. Task 1 is a standard center to reach out task, requiring the subject to move a red circle from the center to one of eight targets (green circle) when prompted. The eight targets are symmetrically spaced along the four quadrants of a circle. Task 2 consists of a (red) rectangular object which the subject can re-size and rotate to match one of eight target (green) rectangles. The eight targets are grouped equivalently to the four target areas in Task 1. With the same mapping function, the set of targets in both tasks require equal input sequences to reach the target from the starting state.

C. Mapping Functions

EMG signals are acquired at 1kHz from four right arm muscles: Biceps Brachii (BB), Triceps Brachii (TB), Flexor Carpi Radialis (FCR) and Extensor Carpi Ulnaris (ECU). The raw EMG signals are pre-processed with full-wave rectification and a low pass filter (2nd order Butterworth, cut-off 8Hz) to remove high frequency noise and obtain a linear envelope of the signal [11]. The processed signal is then transformed through the mapping function to produce the output command.

A mapping function is a 2×4 matrix \mathbf{W}_i , relating a 4×1 vector \mathbf{e} of filtered EMG to a 2×1 vector \mathbf{u} of control outputs:

$$\mathbf{u} = \mathbf{W}_i \mathbf{e}, \quad i \in \{1, 2, 3, 4\} \quad (1)$$

where each \mathbf{W}_i is as defined in Fig. 2. The control outputs are represented visually in 2D control space, with control axes corresponding to the x (horizontal) and y (vertical) velocities of the moving circle in the case of Task 1. For Task 2, the two control axes correspond to the angular velocity and change in size of the rectangle. An activation threshold of

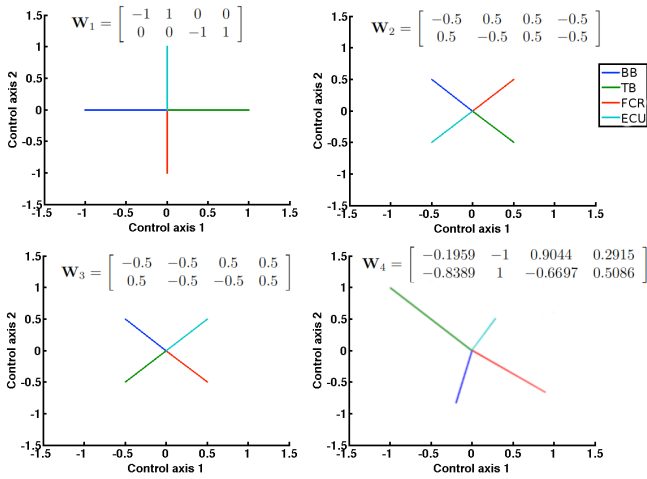


Fig. 2. Mapping of input EMG amplitudes to two output control axes using the mapping function defined in (1).

0.02mV is set for each muscle to nullify any control output at rest.

The mapping function \mathbf{W}_1 should be the most intuitive for subjects, according to [18]. Each set of antagonistic muscles (BB-TB and FCR-ECU) map divergently along one control axis. Mapping functions \mathbf{W}_2 and \mathbf{W}_3 require a combination of two muscles to command direction along a single control axis, with \mathbf{W}_3 encouraging co-contraction of antagonistic muscles. \mathbf{W}_4 is a random matrix with zero row mean so that equal activation of all muscles results in no motion.

D. Trials

A single experiment for a subject consists of 8 trials (four mapping functions for each of the two types of control tasks) performed over two days. The trials are randomly scheduled under the constraints that the tasks alternate and mapping functions are not repeated until every other mapping function has been seen in between. Each mapping function appears only once per day to minimize the feeling of familiarity for each trial. Each trial consists of the scheduled combination of task and mapping function which is unknown to the subject before the trial begins. The subject is assigned to repeatedly transition the red virtual object on the screen from a default initial state to the green target state as quickly as possible. This is repeated for a set of 128 evenly distributed (16 repetitions per target) and randomized sequence of targets, with short 5 second breaks after each successfully reached target. A long break is given after 64 attempts to prevent excessive muscle fatigue. With targets grouped into pairs to represent their respective quadrants, each trial gives 32 data points, representing time taken to reach the final state, for targets in a given quadrant and 32 sets of processed EMG signals, representing the input commands used by the subject while performing the task.

III. RESULTS

Five healthy right-handed subjects (23-30 years old, 1 Female, 4 Male) participated in the experiments. Each gave informed consent according to the procedures approved by

the ASU IRB (Protocol: #1201007252). A qualitative survey was given to the subjects after the experiment to determine their conscious awareness of the differences in each trial. All subjects considered Task 1 to be easier than Task 2, and suggested some mapping functions were easier than others. None realized the same sets of input responses were required to reach the targets in both tasks, although some noticed a few trials required similar muscle activity to move the objects.

Quantitative evaluation looks at performance efficiency and synergy development during operation. An increase in performance efficiency, measured by the time taken to complete a given task, indicates more efficient interaction with the interface to complete tasks quickly. Synergy development confirms convergence toward efficient muscular control of the task-space. Transferring this learning to new control tasks would result in better initial performance and control efficiency.

A. Learning

The assumption behind evaluating learning transfer and synergy development is that learning occurs within each trial when the task and mapping function remain constant. From prior work [17], [18], a chronological plot of time taken to reach each target i ($i \in \{1, 2, 3, 4\}$) for a given trial z ($z \in \{1, 2, \dots, 8\}$) is expected to follow an exponential decay, y_i^z , with respect to the number of attempts x_i^z :

$$y_i^z(x_i^z) = a_i^z 10^{-b_i^z x_i^z} + c_i^z, x \in \{1, 2, \dots, 32\} \quad (2)$$

where $a_i^z > 0$, $b_i^z > 0$, and c_i^z are the initial performance, learning rate, and steady state value, respectively, for trial z and target i . This equation represents an initially high time required (a) to successfully perform any task and a constant exponential decrease (b) towards a final steady-state value (c). Thus, b gives the learning rate for the system. For this analysis, as most subjects are unable to reach steady state in any of the 8 trials, and perfect control of the system would give data points very near 0, each c is assumed to be negligible. Then, to better quantify the results in terms of learning rate, the analysis here plots the data on a logarithmic scale and performs least squares regression to fit a straight line, t_i^z , equivalent to the log of (2):

$$t_i^z(x_i^z) = \log_{10}(y_i^z(x_i^z)) = \log_{10}(a_i^z) - b_i^z x_i^z \quad (3)$$

In (3), steeper slope corresponds to better learning rate. Figure 3 shows an example of a typical data pattern for one quadrant in a given trial, both with original data and the corresponding logarithmic scale. These trends occur for all target quadrants, trials, and subjects, with an overall mean $\bar{b} = 0.0108\text{ms}$ per attempt and standard deviation $\sigma(b) = 0.0074\text{ms}$ per attempt. These learning rates are significant on a student t-test with $p = 3.4570e^{-41}$, consistent with previous findings that learning occurs within each trial.

B. Learning Transfer

With significant learning occurring within each trial, learning transfer can be compared among subsequent trials with

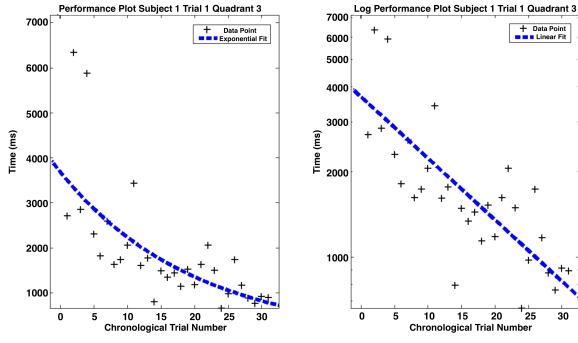


Fig. 3. Typical chronological performance trend for a trial in a given environment, both raw data and logarithmic plots.

either the same control task or mapping function. That is, identify whether the subject is learning to operate the controls of each mapping function irrespective of the control tasks, or whether the subject is learning to interact with each control task better irrespective of the different mapping functions. Learning transfer can be evaluated by analyzing trials chronologically along similar control tasks (Case 1) or mapping functions (Case 2). For a representative subject, two plots are generated to evaluate learning transfer (see Fig. 5). The first plot (Case 1) contains the logarithmic data points for all four trials performed with Task 1, and the second plot (Case 2) contains the logarithmic data points for both trials performed with Mapping Function 2, both plotted horizontally by chronological trial order. Learning transfer is indicated by a smooth transition from the learning curve of one trial, $t_i^{z_0}(x_i^{z_0})$, to the next one, $t_i^{z_0+1}(x_i^{z_0+1})$. In the logarithmic scale, a smooth transition corresponds to two factors, the similarity between $b_i^{z_0}$ and its adjacent $b_i^{z_0+1}$, and the gap between the last data point of one trial, $t_i^{z_0}(32)$ and the first data point in the next trial, $t_i^{z_0}(1)$. Both of these factors are quantified and incorporated into a transition index to determine transition smoothness for a given set of chronologically ordered trials:

- **Root mean squared error (RMSE)** between the line fitted over the entire data (all chronologically-ordered trials) and each t_i^z in the set, shifted to the appropriate order (Fig. 4). A smaller value indicates that each subsequent trial has roughly equal learning rate with increasingly better initial performance.
- **Mean Gap (MG)**, or average difference, between each end point of a previous trial's best fit line ($t_i^{z_0}(32)$) and the start point of the next trial's best fit line ($t_i^{z_0+1}(1)$). A lower value indicates more performance continuity between successive trials.

Both variables are summed to obtain the transition index, with 0 representing a perfect learning transfer:

$$TI(s, i) = \frac{RMSE(s, i)}{n} + MG(s, i) \quad (4)$$

where $TI(s, i)$ is the transition index of subject s at quadrant i , and n is the number of trials used when calculating the RMSE, in order to normalize the index.

The transition index indicates the relative smoothness of the learning transfer between a set of trials, but it does not

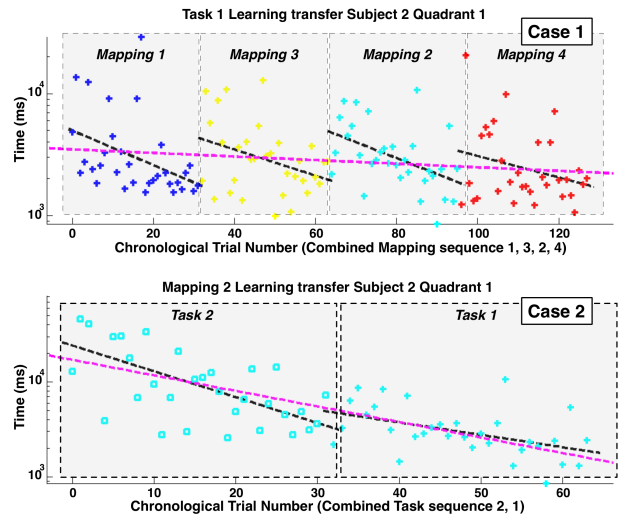


Fig. 4. Example learning transfer plots to evaluate the transition index. The top plot shows poor transition in Case 1, while the bottom plot shows better transition in Case 2. In both cases, the transition index agrees with the amount of learning transfer. Black lines represent the best-fit line for each individual trial, while the magenta line represents best-fit over all trials.

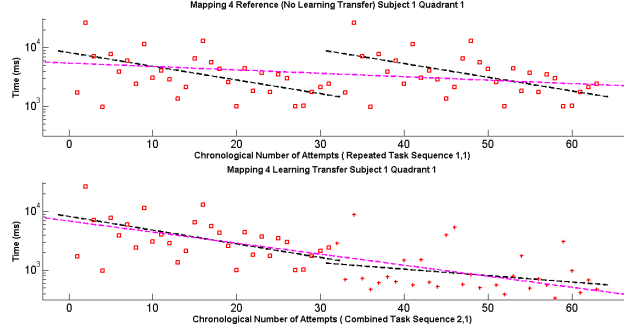


Fig. 5. Example learning transfer plots to evaluate the transfer value. The top plot shows the reference case of no learning transfer, with the first trial repeated, giving $TI_0(1, 1) = 1.4660$. The bottom plot shows the actual trial sequence, with the learning from the first trial transferring to subsequent trials, $TI(1, 1) = 0.3249$. The total transfer value $TV(1, 1) = 1.1411$.

quantify the total amount of transfer. The amount of learning that can be transferred is dependent upon the amount of learning that took place within a given trial. That is, if no learning occurred in the initial trial, there cannot be any learning transferred to subsequent trials, even though it is possible to achieve a perfect transition index. Contrastingly, if the first trial has a high learning rate, more learning can be transferred even without a perfect transition index. Without a reference, the transition index does not quantify the amount of learning that transferred to subsequent trials. If no transfer occurs, all subsequent trials should look identical to the initial trial, regardless of its learning rate. This case is the 0 reference quantifying the maximum amount of transfer possible (see Fig. 5). Therefore, the amount of transfer is a measure of the transition index of the initial trial repeated n times, $TI_0(s, i)$, subtracted by the transition index of the sequence of n trials, $TI(s, i)$:

$$TV(s, i) = TI_0(s, i) - TI(s, i) \quad (5)$$

A higher learning rate in the initial trial, $b_i^{z_0}$, results in a higher TI_0 , indicating more learning is available to be transferred, and vice versa. As $TI \rightarrow 0$, TV approaches its maximum value relative to learning achieved in the first trial. As $TI \rightarrow TI_0$, no learning is transferred, and $TV \rightarrow 0$. $TV < 0$ indicates that the performance in subsequent trials is negatively influenced by or not related to the performance of the first trial. $TV > 0$ indicates at least some learning from the initial trial transferred to the subsequent trials.

The transfer values are calculated for both Case 1 and Case 2 for all subjects. Case 1 has mean transfer $T\bar{V}_1 = 0.0831$ and standard deviation $\sigma(TV_1) = 0.4695$. A student t-test shows insignificant learning transfer when the same task is presented with a different mapping function ($p = 0.2695$). Familiarity with the control task does not help subjects achieve better performance when the mapping function changes. Conversely, Case 2 analysis reveals a significant amount of learning transfer when the same mapping function is presented with a different control task ($T\bar{V}_2 = 0.3177$, $\sigma(TV_2) = 0.4483$, $p = 1.33e^{-8}$). This suggests that the subjects learn new motor controls the first time a mapping function is presented, and retain this learning for at least 24 hours to apply and refine the learning in a completely different task. These results imply that efficient controls can be transferred to any myoelectric interface implementing consistent mapping functions.

C. Synergy Development

Synergy development is analyzed through the evolution of EMG patterns for each individual trial. EMG patterns are initially disorganized while the user identifies the mapping function, but after many trials the EMG pattern becomes more structured, signifying the development of a new synergy. EMG patterns between subjects have more similarities as the number of attempts at a given target increases (see Fig. 6), indicating convergence to a more efficient control.

The increasing similarities can be quantified using mutual information, a general measure of dependencies between variables based on information theory [24]. Briefly, given a discretized system F of M_F states, where each state f_i occurs with probability $p(f_i)$, the expected information gain from a measurement of value f_i is the entropy $H(F)$ of the system [24]. Two discrete systems, F and G , have joint entropy $H(F, G)$. Given that $H(F, G) \leq H(F) + H(G)$, the mutual information between F and G is

$$I(F, G) = H(F) + H(G) - H(F, G). \quad (6)$$

So long as both F and G have some uncertainty, as in EMG sequences, normalized mutual information (NMI) is found by:

$$NMI(F, G) = \sqrt{\frac{I(F, G)^2}{H(F)H(G)}}, H(F) > 0, H(G) > 0 \quad (7)$$

with $NMI = 0$ for independent F and G and $NMI = 1$ for perfectly correlated F and G . To use (7) to evaluate synergy development, the time-varying sequence of EMG data is first

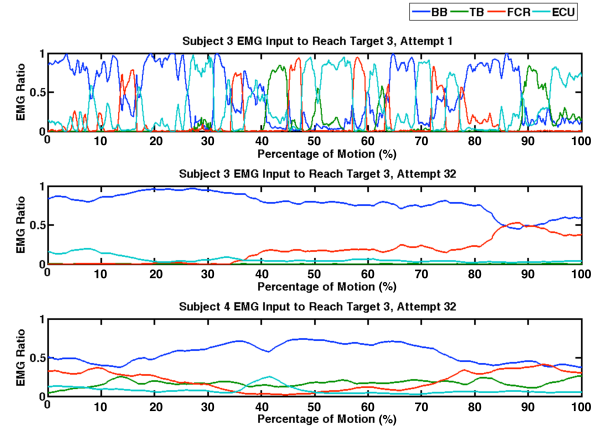


Fig. 6. Example EMG sequence for 3 attempts to reach a given target. The top plot shows a scrambled EMG signal on a subject’s first attempt to reach the target. The middle plot shows a more structured EMG signal on the subject’s last attempt in the same trial. The bottom plot shows a similar EMG signal on another subject’s last attempt for the same trial combination. The similarity of the EMG signals after 32 attempts reveals a common synergy developing between subjects.

normalized with respect to completion time and total effort put into the system for each target attempt. The signal is first resampled along the time axis with cubic interpolation to a common set of 500 samples. Then the EMG signal for each muscle at each sample is normalized with respect to the sum of all EMG signals at that sample. The resulting signal contains percentage of motion completeness along one axis and EMG ratios along the other (see Fig. 6).

When comparing adjacent target attempts for a given trial, NMI shows a linear trend with positive slope. For all trials and subjects, the mean slope for all best-fit lines is 0.0011 per attempt, which is significant on a student t-test ($p = 2.6696e^{-23}$). Comparing NMI across all subjects for each trial combination reveals an identical linear trend. For each attempt in a given trial, NMI is calculated between all combinations of two subjects. The mean NMI between all subjects is plotted against the number of attempts for each trial (see Fig. 7). The mean slope m of the best fit line for all trials is significantly positive ($\bar{m} = 0.0010$ per attempt, $\sigma(m) = 0.0005$, $p = 7.1228e^{-12}$). This confirms that the EMG signals of all subjects are slowly converging towards a common signal pattern, supporting the hypothesis that all subjects are developing the same set of basis synergies while learning the inverse model of the mapping function.

IV. CONCLUSIONS

This paper investigates the transfer of learning and population-wide synergy development for efficient performance in myoelectric controlled interfaces. The results reveal a significant learning transfer when a new control task is presented to a subject using the same mapping function as a previous control task. This gives evidence that subjects do not only learn those mappings between their actions and the control task, but they can retain this learning and generalize it to different control tasks resulting in better initial performance and control efficiency. Moreover, comparison of EMG signals for all subjects show that the signals become

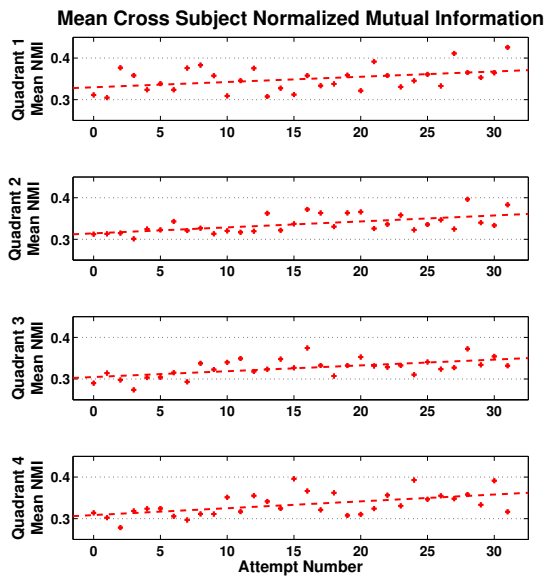


Fig. 7. Example Normalized Mutual Information trends.

significantly more similar as subjects spend more time using a specific mapping function and control task. This suggests a development of population-wide synergies while learning the inverse model of a given decoder, confirming convergence towards efficient muscular control of the task-space.

These two findings support the idea of the human embedded control of devices using myoelectric interfaces, which can result in a paradigm shift in the research field of neuro-prosthetics. More specifically, results show that humans can be trained to control different tasks by learning new motor controls mapping directly to the control axes of the tasks (i.e. embedded control). The implications of this method are vast, since it means that myoelectric controlled interfaces can extend beyond anthropomorphic controls and user-specific decoders. Instead, humans can learn to efficiently control the interface through practice and synergy development, opening new avenues and capabilities for the intelligent control of myoelectric controlled robotic systems.

REFERENCES

- [1] S. Bitzer and P. van der Smagt, "Learning EMG control of a robotic hand: towards active prostheses," in *Robotics and Automation, 2006. ICRA 2006. Proceedings 2006 IEEE International Conference on*. IEEE, may 2006, pp. 2819–2823.
- [2] C. Castellini, A. E. Fiorilla, and G. Sandini, "Multi-subject / Daily-Life Activity EMG-based control of mechanical hands," *Journal of Neuroengineering and Rehabilitation*, vol. 6, no. 41, 2009.
- [3] P. K. Artemiadis and K. J. Kyriakopoulos, "EMG-Based Position and Force Estimates in Coupled Human-Robot Systems: Towards EMG-Controlled Exoskeletons," in *Experimental Robotics*, ser. Springer Tracts in Advanced Robotics, O. Khatib, V. Kumar, and G. J. Pappas, Eds. Springer Berlin Heidelberg, 2009, vol. 54, pp. 241–250.
- [4] C. Zhu, S. Shimazu, M. Yoshioka, and T. Nishikawa, "Power assistance for human elbow motion support using minimal EMG signals with admittance control," in *Mechatronics and Automation (ICMA), 2011 International Conference on*. IEEE, Aug 2011, pp. 276–281.
- [5] T. S. Saponas, D. S. Tan, D. Morris, and R. Balakrishnan, "Demonstrating the feasibility of using forearm electromyography for muscle-computer interfaces," in *Proceedings of the SIGCHI Conference on Human Factors in Computing Systems*, ser. CHI '08, ACM. New York, NY, USA: ACM, 2008, pp. 515–524.
- [6] P. K. Artemiadis and K. J. Kyriakopoulos, "A Switching Regime Model for the EMG-Based Control of a Robot Arm," *IEEE Transactions on Systems, Man, and Cybernetics, Part B: Cybernetics*, vol. 41, no. 1, pp. 53–63, Feb 2011.
- [7] M. S. Erkilinc and F. Sahin, "Camera control with EMG signals using Principal Component Analysis and support vector machines," in *Systems Conference (SysCon), 2011 IEEE International*. IEEE, Apr 2011, pp. 417–421.
- [8] J. Vogel, C. Castellini, and P. van der Smagt, "EMG-based teleoperation and manipulation with the DLR LWR-III," in *Intelligent Robots and Systems (IROS), 2011 IEEE/RSJ International Conference on*, sept. 2011, pp. 672–678.
- [9] A. B. Ajiboye and R. F. Weir, "Muscle synergies as a predictive framework for the EMG patterns of new hand postures," *Journal of Neural Engineering*, vol. 6, no. 3, p. 036004, Jun 2009.
- [10] F. Orabona, C. Castellini, B. Caputo, A. Fiorilla, and G. Sandini, "Model adaptation with least-squares SVM for adaptive hand prosthetics," in *Robotics and Automation, 2009. ICRA '09. IEEE International Conference on*. IEEE, May 2009, pp. 2897–2903.
- [11] F. E. Zajac, "Muscle and tendon: properties, models, scaling, and application to biomechanics and motor control," *Stanford University*, vol. 17, pp. 359–411, 1989.
- [12] C. Cipriani, F. Zaccone, S. Micera, and M. Carrozza, "On the Shared Control of an EMG-Controlled Prosthetic Hand: Analysis of User-Prosthesis Interaction," *Robotics, IEEE Transactions on*, vol. 24, no. 1, pp. 170–184, Feb 2008.
- [13] P. Nilas, P. Rani, and N. Sarkar, "An innovative high-level human-robot interaction for disabled persons," in *Robotics and Automation, 2004. Proceedings. ICRA '04. 2004 IEEE International Conference on*, vol. 3. IEEE, april-1 may 2004, pp. 2309–2314 Vol.3.
- [14] J. P. Cunningham, P. Nuyujukian, V. Gilja, C. A. Chestek, S. I. Ryu, and K. V. Shenoy, "A closed-loop human simulator for investigating the role of feedback control in brain-machine interfaces," *Journal of Neurophysiology*, vol. 105, no. 4, pp. 1932–1949, Apr 2011.
- [15] R. Hélot, K. Ganguly, J. Jimenez, and J. M. Carmena, "Learning in Closed-Loop Brain-Machine Interfaces: Modeling and Experimental Validation," *IEEE Transactions on Systems, Man, and Cybernetics*, vol. 40, p. 11, 2010.
- [16] S. Kim, S. JD, H. LR, D. JP, and B. MJ, "Neural control of computer cursor velocity by decoding motor cortical spiking activity in humans with tetraplegia," *J Neural*, vol. 5, p. 22, 2008.
- [17] S. M. Chase, A. B. Schwartz, and R. E. Kass, "Bias, optimal linear estimation, and the differences between open-loop simulation and closed-loop performance of spiking-based brain computer interface algorithms," *Neural Networks*, vol. 22, no. 9, pp. 1203–1213, Nov 2009.
- [18] S. M. Radhakrishnan, S. N. Baker, and A. Jackson, "Learning a novel myoelectric-controlled interface task," *J Neurophysiol*, vol. 1, p. 47, 2008.
- [19] T. Pistohl, C. Cipriani, A. Jackson, and K. Nazarpour, "Abstract and Proportional Myoelectric Control for Multi-Fingered Hand Prostheses," *Annals of Biomedical Engineering*, vol. 41, no. 12, pp. 2687–2698, Dec 2013.
- [20] A. d'Avella and F. Lacquaniti, "Control of reaching movements by muscle synergy combinations," *Frontiers in Computational Neuroscience*, 2013.
- [21] P. Artemiadis and K. Kyriakopoulos, "EMG-Based Control of a Robot Arm Using Low-Dimensional Embeddings," *Robotics, IEEE Transactions on*, vol. 26, no. 2, pp. 393–398, april 2010.
- [22] K. Nazarpour, A. Barnard, and A. Jackson, "Flexible Cortical Control of Task-Specific Muscle Synergies," *Journal of Neuroscience*, vol. 32, no. 36, pp. 12 349–12 360, Sep 2012.
- [23] [Online]. Available: <http://www.opengl.org>
- [24] R. Steuer, J. Kurths, C. Daub, J. Weise, and J. Selbig, "The mutual information: Detecting and evaluating dependencies between variables," *Bioinformatics*, vol. 18 Suppl.2, pp. S231–S240, 2002.